

# ***Ab initio* calculations of energy levels in Be-like xenon: strong interference between electron-correlation and QED effects**

A. V. Malyshev,<sup>1</sup> D. A. Glazov,<sup>1</sup> Y. S. Kozhedub,<sup>1</sup> I. S. Anisimova,<sup>1</sup>  
M. Y. Kaygorodov,<sup>1</sup> V. M. Shabaev,<sup>1</sup> and I. I. Tupitsyn<sup>1</sup>

<sup>1</sup>*Department of Physics, St. Petersburg State University, Universitetskaya 7/9, 199034 St. Petersburg, Russia*

High-precision QED calculations of the ground and singly excited energy levels in Be-like xenon are performed. The close levels of the same symmetry which are strongly mixed by the electron-electron interaction are treated within the QED perturbation theory for quasidegenerate states. The contributions of all the Feynman diagrams up to the second order are taken into account. The many-electron QED effects are rigorously evaluated in the framework of the extended Furry picture to all orders in the nuclear-strength parameter  $\alpha Z$ . The higher-order electron-correlation effects are considered within the Breit approximation. The nuclear recoil effect is accounted for as well. The most accurate theoretical predictions for the binding and excitation energies are obtained. These results deviate from the most precise experimental value by  $3\sigma$  but perfectly agree with a more recent measurement.

Be-like ions represent the simplest example of atomic systems with more than one electron in a valence shell. Electromagnetic interaction of the  $L$ -shell electrons, combined with intershell correlation effects, leads to a strong mixing of the close energy levels of the same symmetry. On the other hand, precise calculations of highly charged Be-like ions must include QED effects, which are of the same order of magnitude as in He- and Li-like ions (see, e.g., the recent review [1] and references therein). Therefore, highly charged Be-like ions pose a serious challenge to atomic structure calculations within the framework of bound-state QED. Despite numerous relativistic calculations of the energy levels in these systems [2–16], the QED effects have been included at best within some one-electron approximations only. Different theoretical approaches show significant scatter of the results when compared with the available experimental data [17–28]. The many-electron QED effects for the ground state of Be-like ions were evaluated in our recent works [29, 30], where the calculations were performed using the QED perturbation theory for a single level. However, due to the proximity of all the  $n = 2$  levels, including the ground state, the accuracy of this evaluation remains unclear, unless the calculations based on *ab initio* QED approach for quasidegenerate states are performed. The present work is intended to solve this long-standing and extremely difficult problem. The development of the rigorous QED theory for the high-precision calculations of the ground and singly excited states in Be-like ions is the primary goal of this study. To the best of our knowledge, the QED calculations of the quasidegenerate states at such a level have never been performed previously for the systems with more than two electrons. Moreover, the three-dimensional model subspace of quasidegenerate levels, which we employ in the present paper, is also considered for the first time in the framework of *ab initio* approach. It is the application of such sophisticated methods that allows us to accurately address an issue of strong interference between electron-electron interaction and QED effects.

The natural zeroth-order approximation for the sys-

tematic QED description of highly charged ions is provided by the Dirac equation

$$[\boldsymbol{\alpha} \cdot \mathbf{p} + \beta m + V] \psi_n = \varepsilon_n \psi_n. \quad (1)$$

By substituting the Coulomb potential of the nucleus  $V_{\text{nuc}}$  as the binding potential  $V$  in Eq. (1) one comes to the Furry picture of QED [31]. The electron-nucleus interaction is taken into account to all orders in  $\alpha Z$  in this way ( $\alpha$  is the fine-structure constant,  $Z$  is the nuclear charge number). In order to partially account for the electron-electron interaction effects from the very beginning, the initial approximation can be modified by adding some local screening potential,  $V = V_{\text{nuc}} + V_{\text{scr}}$ . This corresponds to the extended version of the Furry picture [32–43]. The remaining part of the interelectronic interaction as well as the interaction with the quantized electromagnetic field are to be considered within appropriate perturbation theory (PT).

Standard nondegenerate PT suits well for single (isolated) levels, such as the ground state  $1s^2$  of He-like ions [44], or when one studies, e.g., the fine-structure splitting  $2p_{j-2s}$  in Li-like ions [40, 41]. However, considering more complicated systems or excited states one inevitably encounters close levels with the same symmetry which are mixed strongly by the electron-electron interaction. Application of the extended Furry picture allows one to lift the degeneracy in some cases. Nevertheless, the proper treatment of these systems requires employing PT for quasidegenerate levels. Both types of the QED perturbation series can be conveniently constructed in the framework of the two-time Green's function (TTGF) method [45]. For a set of  $s$  quasidegenerate levels, the TTGF method implies the evaluation of the  $s \times s$  matrix  $H$  which acts in the model subspace  $\Omega$  spanned by the unperturbed wave functions of the states under consideration. The energies can be obtained by diagonalizing the matrix  $H$ . PT for a single level corresponds to  $s = 1$ .

In the present work, we aim at the *ab initio* evaluation of the ground and singly excited energy levels in

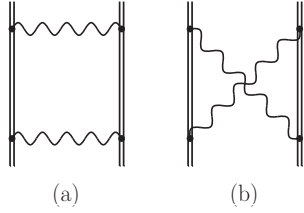


FIG. 1. Two-photon exchange diagrams.

Be-like xenon. Despite the fact that our calculations are fully relativistic, we employ the  $LS$ -coupling notations. The excited states with the total angular momentum equal to  $J = 0$  and  $J = 2$ , namely  $2s2p^3P_0$  and  $2s2p^3P_2$  (here and in what follows, the  $K$  shell is omitted for brevity), are considered as the single levels. The corresponding unperturbed wave functions in the  $jj$  coupling read as  $(2s2p_{1/2})_0$  and  $(2s2p_{3/2})_2$ , respectively. The states  $2s2p^3P_1$  and  $2s2p^1P_1$  with  $J = 1$  are studied within the two approaches: (a) as the isolated levels, starting from the initial approximations  $(2s2p_{1/2})_1$  and  $(2s2p_{3/2})_1$ ; (b) as a pair of quasidegenerate levels within the two-dimensional subspace  $\Omega$ . Finally, the binding energy of the ground  $2s2s^1S_0$  state is evaluated by means of three independent approaches: (a) as the isolated  $(2s2s)_0$  level; (b) as one of the two quasidegenerate levels,  $(2s2s)_0$  and  $(2p_{1/2}2p_{1/2})_0$ , within the two-dimensional subspace  $\Omega$ ; (c) as one of the three quasidegenerate levels, including the  $(2p_{3/2}2p_{3/2})_0$  configuration, for which the mixing coefficient can be even larger than for  $(2p_{1/2}2p_{1/2})_0$  [2, 46]. The approach (a) for the ground state reproduces the one which we have used in Ref. [29]. In the Coulomb potential, the unperturbed levels forming the quasidegenerate subspaces are split only by the nuclear-size and relativistic effects.

Let us briefly formulate our approach. In order to derive all the relevant calculation formulas, we start with the formalism in which the closed  $1s^2$  shell is regarded as belonging to the vacuum [45], and there are two  $L$ -shell “valence” electrons. The redefinition of the vacuum is carried out by changing the sign before  $i0$  in the electron-propagator denominators corresponding to the closed shell, i.e., the standard Green’s function  $G$  is replaced as follows:

$$G(\omega) \equiv \sum_n \frac{|n\rangle\langle n|}{\omega - \varepsilon_n + i\varepsilon_n 0} \rightarrow \sum_n \frac{|n\rangle\langle n|}{\omega - \varepsilon_n + i\eta_n 0}, \quad (2)$$

where  $\eta_n = \varepsilon_n - \varepsilon_F$ , and  $\varepsilon_F$  is the Fermi energy. The Fermi energy is chosen to be higher than the energy of the closed-shell electrons but lower than the valence-electron energy. In this formalism, the one- and two-loop one-electron Feynman diagrams include the contributions describing the interaction between one valence electron and the closed shell. These contributions can be separated by considering the difference with the standard definition of the vacuum. For instance, the first-order self-energy and vacuum-polarization diagrams for the valence state  $|v\rangle$  lead to the one-photon exchange contribution

$$\Delta E_{\text{int}}^{(1)} = \sum_c [I_{vcvc}(0) - I_{cvvc}(\varepsilon_v - \varepsilon_c)], \quad (3)$$

where  $I_{abcd}(\omega) = \langle ab|I(\omega)|cd\rangle$ ,  $I(\omega) = e^2\alpha_1^\mu\alpha_2^\nu D_{\mu\nu}(\omega)$ ,  $\alpha^\mu = (1, \boldsymbol{\alpha})$ , and  $D_{\mu\nu}(\omega)$  is the photon propagator. We stress that the treatment of the one-electron diagrams does not depend on the type of PT. By employing this formalism, we obtain the well-known expressions for the intershell-interaction corrections derived previously for Li-like systems, see, e.g., Refs. [41, 47–49].

Now we turn to the discussion of the two-electron diagrams within the formalism with the redefined vacuum. These diagrams contain the three-electron contributions corresponding to the interaction of both the valence electrons with the  $1s^2$  core. In case of He-like ions and two-dimensional subspace  $\Omega$ , the formal expressions for the second-order two-electron contributions were derived within the TTGF method in Refs. [50–52], see also Ref. [53]. In the present work, we have generalized these expressions to deal with an arbitrary number of quasidegenerate levels. The most complicated and time-consuming is the derivation of the formulas for the two-photon exchange diagrams in Fig. 1. We restrict our consideration only to the contribution of the ladder diagram in Fig. 1(a). This contribution is naturally divided into the reducible (“red”) and irreducible (“irr”) parts. The reducible part involves the terms with the intermediate states coinciding with the quasidegenerate levels under consideration, while the irreducible part corresponds to the remainder. The reducible part is not affected by the redefinition of the vacuum, and its contribution to  $H$ , arising from the interaction between the valence electrons, reads as

$$H_{ik}^{\text{red}} = -\frac{1}{2} \sum_P (-1)^P \sum_{n_1 n_2}^{E_n^{(0)}=E_1^{(0)}\dots E_s^{(0)}} \frac{i}{2\pi} \int_{-\infty}^{\infty} d\omega \left[ \frac{I_{Pi_1Pi_2n_1n_2}(\omega - \varepsilon_{Pi_1}) I_{n_1n_2k_1k_2}(\varepsilon_{k_1} - \omega)}{(\omega - \varepsilon_{n_1} - i0)(\omega + \varepsilon_{n_2} - \bar{E}_{ik}^{(0)} - i0)} + \{1 \leftrightarrow 2\} \right], \quad (4)$$

where the indices  $i$  and  $k$  enumerate the quasidegenerate states,  $P$  is the permutation operator,  $E_n^{(0)} = \varepsilon_{n_1} + \varepsilon_{n_2}$ ,  $\bar{E}_{ik}^{(0)} = (E_i^{(0)} + E_k^{(0)})/2$ , and  $\{1 \leftrightarrow 2\}$  means the expression with the transposed indices 1 and 2. The contribution of the irreducible part of the ladder diagram within the employed formalism can be expressed as follows:

$$\tilde{H}_{ik}^{\text{irr}} = \frac{1}{2} \sum_P (-1)^P \sum_{n_1 n_2}^{E_n^{(0)} \neq E_1^{(0)} \dots E_s^{(0)}} \frac{i}{2\pi} \int_{-\infty}^{\infty} d\omega \left[ \frac{I_{Pi_1Pi_2n_1n_2}(\omega - \varepsilon_{Pi_1}) I_{n_1n_2k_1k_2}(\varepsilon_{k_1} - \omega)}{(\omega - \varepsilon_{n_1} + i\eta_{n_1} 0)(\bar{E}_{ik}^{(0)} - \omega - \varepsilon_{n_2} + i\eta_{n_2} 0)} + \{1 \leftrightarrow 2\} \right]. \quad (5)$$

We readily extract the desired three-electron contribution from Eq. (5)

$$\delta H_{ik}^{3\text{el}} = -\frac{1}{2} \sum_P (-1)^P \sum_c \sum_n \frac{1}{\bar{E}_{ik}^{(0)} - \varepsilon_c - \varepsilon_n} \left[ I_{Pi_1 Pi_2 nc} (\bar{E}_{ik}^{(0)} - \varepsilon_c - \varepsilon_{Pi_1}) I_{nck_1 k_2} (\varepsilon_{k_1} + \varepsilon_c - \bar{E}_{ik}^{(0)}) \right. \\ \left. + I_{Pi_1 Pi_2 nc} (\varepsilon_c - \varepsilon_{Pi_2}) I_{nck_1 k_2} (\varepsilon_{k_2} - \varepsilon_c) + \{1 \leftrightarrow 2\} \right]. \quad (6)$$

The total three-electron contribution can be obtained by studying the crossed diagram in Fig. 1(b) and the two-electron self-energy and vacuum-polarization graphs.

By considering the one- and two-electron diagrams in the formalism with the redefined vacuum, we take into account all the necessary contributions describing the interaction between the  $L$  and  $K$  shells. In order to evaluate the total binding energies of Be-like ions, we have to add the QED contributions corresponding to the  $1s^2$  core. This issue is discussed in details, e.g., in Refs. [53, 54]. As a result, our numerical approach rigorously takes into account all the contributions of the first and second orders of QED PT. The electron-correlation contributions due to the exchange by three or more photons are accounted for within the Breit approximation in the present work. The corresponding calculations are based on the Dirac–Coulomb–Breit (DCB) Hamiltonian and performed by means of the large-scale configuration-interaction (CI) method in the basis of the Dirac–Sturm orbitals [55–57]. The procedure how to merge the QED calculations with the higher-order interelectronic-interaction contributions in case of quasidegenerate levels was suggested first in Ref. [54] and described in more details in Ref. [53]. Finally, we account for the nuclear recoil and nuclear polarization effects which lie beyond the external-field approximation, that is beyond the Furry picture.

Let us now turn to the discussion of the numerical results. In Table I, we present the binding energies of the ground and singly excited states in Be-like xenon. The calculations are performed starting from the Coulomb potential as well as within the extended Furry picture. In the latter case, the core-Hartree (CH) and local Dirac–Fock (LDF) screening potentials are incorporated in Eq. (1). The description and applications of these potentials can be found, e.g., in Refs. [34, 43, 58]. For the nuclear charge distribution, the Fermi model is used. The root-mean-square radius and the nuclear mass of the isotope  $^{132}\text{Xe}$  are taken as in Ref. [59].

As noted above, for the ground and  $J = 1$  states we construct the alternative perturbation series for both the single and the quasidegenerate levels. The type of PT is shown in the first column, where the size of the subspace  $\Omega$  is indicated. The columns labeled with A, B, C, and D demonstrate how the energies change when we successively take into account different contributions. In the column A, we present the values obtained within the Breit approximation by means of the CI method.

From Table I, one can see that for the specific potential these results do not depend on the size of  $\Omega$ . We note that the  $1 \times 1$  values are just the CI energies, whereas the  $2 \times 2$  and  $3 \times 3$  values are obtained as the eigenvalues of the matrices  $H$  which are constructed based on the CI calculations in accordance with the prescriptions from Ref. [53]. The energies for the specific subspace  $\Omega$  in the column A vary slightly from the potential to potential. This variation is caused by the dependence of the positive-energy-states projectors in the DCB Hamiltonian on the initial approximation in our approach, see the discussion, e.g., in Refs. [53, 57].

The results in the column B are obtained by adding the first-order QED contributions, namely the self energy, vacuum polarization, and frequency-dependent correction of the one-photon exchange contribution, as well as the nuclear recoil and nuclear polarization contributions. We stress that for the quasidegenerate levels the inclusion of the terms is not quite additive because of the mixing. One can see that the results for different potentials demonstrate significant scatter. The scatter can be reduced by considering the second-order QED corrections. This is done in the column C, where we add the contributions of the two-electron self-energy and vacuum-polarization diagrams, the nontrivial QED part of the two-photon exchange contribution (beyond the Breit approximation), and the two-loop one-electron corrections. The difference between the calculations with the Coulomb, CH, and LDF potentials indeed decreases going from B to C. The values in the column C obtained for the screening potentials are shifted slightly with respect to the Coulomb ones. This results from a rearrangement of the perturbation series within the extended Furry picture.

From the column C, it is seen that the energy of the ground  $2s2s\ ^1S_0$  state considerably shifts as we pass from  $1 \times 1$  to  $2 \times 2$ . However, the value of this shift is almost independent on the initial approximation. The shift is explained by the accurate treatment of the mixing of the states within the model subspace. When we extend  $\Omega$  by including the  $(2p_{3/2}2p_{3/2})_0$  configuration, the ground-state energy acquires an additional shift which is smaller by an order of magnitude. The uncertainties of these calculations are determined, in particular, by the uncalculated screened QED contributions of the second order in  $1/Z$ . Nowadays, these corrections are inaccessible by the rigorous QED methods. We can estimate them approximately employing

TABLE I. Binding energies (with the opposite sign) of the ground and singly excited states in Be-like xenon (in eV). Comparison of the different approaches: A, B, C, and D. See the text for details.

$\Omega$	$V_{\text{eff}}$	A	B	C	D
$2s2s^1S_0$					
$1 \times 1$	Coul	101 071.884	100 970.193	100 973.026	—
	CH	101 071.948	100 973.924	100 972.977	100 973.569
	LDF	101 071.928	100 973.451	100 972.981	100 973.400
$2 \times 2$	Coul	101 071.884	100 970.443	100 973.244	100 973.263
	CH	101 071.948	100 974.157	100 973.194	100 973.246
	LDF	101 071.928	100 973.682	100 973.198	100 973.237
$3 \times 3$	Coul	101 071.884	100 970.487	100 973.278	100 973.240
	CH	101 071.948	100 974.199	100 973.229	100 973.241
	LDF	101 071.928	100 973.724	100 973.233	100 973.236
$2s2p^3P_0$					
$1 \times 1$	Coul	100 961.328	100 866.432	100 868.743	100 868.704
	CH	100 961.373	100 869.738	100 868.699	100 868.710
	LDF	100 961.356	100 869.227	100 868.703	100 868.705
$2s2p^3P_1$					
$1 \times 1$	Coul	100 938.533	100 843.637	100 845.987	100 845.930
	CH	100 938.579	100 846.944	100 845.941	100 845.935
	LDF	100 938.562	100 846.433	100 845.946	100 845.930
$2 \times 2$	Coul	100 938.533	100 843.635	100 845.975	100 845.935
	CH	100 938.579	100 846.941	100 845.930	100 845.941
	LDF	100 938.562	100 846.430	100 845.934	100 845.935
$2s2p^3P_2$					
$1 \times 1$	Coul	100 596.593	100 501.446	100 503.789	100 503.754
	CH	100 596.656	100 504.784	100 503.744	100 503.757
	LDF	100 596.637	100 504.272	100 503.748	100 503.751
$2s2p^1P_1$					
$1 \times 1$	Coul	100 533.196	100 438.050	100 440.465	100 440.441
	CH	100 533.262	100 441.390	100 440.416	100 440.445
	LDF	100 533.242	100 440.878	100 440.420	100 440.439
$2 \times 2$	Coul	100 533.197	100 438.053	100 440.477	100 440.437
	CH	100 533.262	100 441.392	100 440.428	100 440.439
	LDF	100 533.242	100 440.880	100 440.432	100 440.434

the model Lamb-shift (QEDMOD) operator which has been suggested recently in Refs. [60, 61] and successfully applied to the QED calculations in various atomic systems [57, 62–67]. In order to estimate the screened QED effects of the second order in  $1/Z$ , we have introduced the QEDMOD operator into Eq. (1) and evaluated the two-photon exchange contribution in the Breit approximation using the related one-electron basis. The correction of interest was obtained by subtracting the corresponding contribution calculated without the QEDMOD operator. The binding energies with these corrections included are shown in the column D. One can see that the  $1 \times 1$  values for the  $2s2s^1S_0$  state tend

to the eigenvalues of the matrices  $H$ . However, the discrepancy of the results for two screening potentials is large. Within nondegenerate PT, the higher-order QED effects contribute significantly, and their contribution can not be neglected. On the other hand, in the column D the difference between the  $2 \times 2$  and  $3 \times 3$  values decreases, and the Coulomb results become closer to the ones obtained for the screening potentials. Based on all the results given in Table I, we conclude that the  $3 \times 3$  subspace  $\Omega$  is sufficient for the proper treatment of the electron-correlation and QED effects on the ground-state binding energy. As for the  $J = 1$  states, the situation, in principal, is the same. However, the mixing is less pronounced than for the ground state.

The values shown in the column D of Table I for the LDF potential and the maximum size of the subspace  $\Omega$  are employed as the final results. The uncertainties are obtained by summing quadratically several contributions. First, in addition to the numerical errors, we take into account the uncertainties of the nuclear-size effect and of the two-loop one-electron corrections [59]. Second, we estimate the uncalculated higher-order QED contributions through several means. The QED corrections to the electron-correlation effects of third and higher orders are estimated according to the procedure from Ref. [53]. The screening of the two-loop contributions is estimated by multiplying the corresponding term for  $1s$  by the conservative factor  $2/Z$ . We take into account the scatter of the results obtained for the different potentials as well. Finally, having in mind that the calculations of the screened QED effects of the second order in  $1/Z$  in the column D are approximate, we take the corresponding correction with the 100% uncertainty. As a result, for the ground-state binding energy we obtain  $E[2s2s^1S_0] = -100973.236(44)$  eV, which deviates from  $-100972.921(85)$  eV [29]. We have to admit that the higher-order QED effects have been underestimated in our previous calculations. We note that the current  $1 \times 1$  value presented in the column C for the LDF potential, which is obtained within the approach closest to Ref. [29], is also shifted with respect to the old one within the designated error bar. The reasons are in the different approach to evaluate the higher-order interelectronic-interaction contributions within the Breit approximation, the revised two-loop one-electron corrections, and the updated values of the fundamental constants [68]. The binding energies of the singly excited levels are  $E[2s2p^3P_0] = -100 868.705(42)$  eV,  $E[2s2p^3P_1] = -100 845.935(42)$  eV,  $E[2s2p^3P_2] = -100 503.751(42)$  eV, and  $E[2s2p^1P_1] = -100 440.434(42)$  eV.

The obtained binding energies are used to evaluate the excitation energies for the  $2s2p^{2S+1}P_J$  states presented in Table II. The uncertainties are estimated similarly to the binding energies. In Table II, we compare our excitation energies with the results of the previous relativistic calculations and recent measurements. In Ref. [57], these energies were evaluated by means of



TABLE II. Excitation energies from the ground  $2s^2\ ^1S_0$  to  $2s2p^{2S+1}P_J$  states in  $\text{Xe}^{50+}$  (in eV).

$2s2p\ ^3P_0$	$2s2p\ ^3P_1$	$2s2p\ ^3P_2$	$2s2p\ ^1P_1$	Year	Reference
Theory					
104.531(9)	127.300(9)	469.484(7)	532.802(7)	2020	This work
104.5(25)	127.3(25)	469.6(25)	532.9(25)	2019	Kaygorodov <i>et al.</i> [57]
104.475	127.282	469.449	532.877	2008	Cheng <i>et al.</i> [11]
104.663	127.475	470.004	533.401	2005	Gu [9]
	127.168	469.25	532.62	2000	Safronova [7]
	127.301		532.854	1997	Chen & Cheng [6]
104.482	127.267	469.386	532.759	1996	Safronova <i>et al.</i> [5]
103.722	126.846	468.338	532.766	1979	Cheng <i>et al.</i> [3]
Experiment					
	127.269(46)	469.474(81)	532.801(16)	2015	Bernhardt <i>et al.</i> [28]
	127.260(26)			2005	Feili <i>et al.</i> [26]
	127.255(12)			2003	Träbert <i>et al.</i> [24]
	127.3(3)			1992	Büttner <i>et al.</i> [21]
	126.6(5)			1991	Möller <i>et al.</i> [20]
	126.6(5)			1990	Träbert <i>et al.</i> [19]
	126.4(6)			1989	Möller <i>et al.</i> [18]

the CI+QEDMOD method, and the uncertainties were estimated in a rather conservative way. However, the comparison with the results of the present work shows that the accuracy of this approach is at least one order of magnitude higher. As for the experiments, our results are in perfect agreement with the most recent measurements performed in Ref. [28], especially for the  $2s2p\ ^1P_1$  state, for which the experimental uncertainty is minimal. On the other hand, the most precise measurement for the  $2s2p\ ^3P_1$  state [24] deviates from our result by almost 4 times the experimental uncertainty and by 5 times our theoretical uncertainty. The reason of this discrepancy is unclear to us.

To summarize, *ab initio* QED calculations of the binding energies of the ground and singly excited states in Be-like xenon have been performed with the most advanced methods available to date. The calculations merge the rigorous QED treatment up to the second-order contributions and the higher-order

electron-correlation effects evaluated within the Breit approximation. For the first time, the ground state as well as the states with the total angular momentum equal to 1 are treated by means of perturbation theory for quasidegenerate levels. As a result, we have obtained the most precise theoretical predictions for the energy levels and  $\Delta n = 0$  intra- $L$ -shell excitation energies, which are in perfect agreement with the most recent measurements [28]. Meanwhile, some discrepancy with the previous experiment [24] is found. New measurements with Be-like xenon and other Be-like ions are in demand.

This work was supported by the grant of the President of the Russian Federation (Grant No. MK-1459.2020.2). A.V.M., M.Y.K., and V.M.S. acknowledge the support from the Foundation for the Advancement of Theoretical Physics and Mathematics “BASIS”. D.A.G. acknowledges the support by RFBR (Grant No. 19-02-00974). The work of I.I.T. was supported by RFBR (Grant No. 18-03-01220).

- 
- [1] P. Indelicato, J. Phys. B: At. Mol. Opt. Phys. **52**, 232001 (2019).
  - [2] L. Armstrong, W. R. Fielder, and D. L. Lin, Phys. Rev. A **14**, 1114 (1976).
  - [3] K. T. Cheng, Y. K. Kim, and J. P. Desclaux, At. Data Nucl. Data Tables **24**, 111 (1979).
  - [4] X.-W. Zhu and K. T. Chung, Phys. Rev. A **50**, 3818 (1994).
  - [5] M. S. Safronova, W. R. Johnson, and U. I. Safronova, Phys. Rev. A **53**, 4036 (1996).
  - [6] M. H. Chen and K. T. Cheng, Phys. Rev. A **55**, 166 (1997).
  - [7] U. I. Safronova, Mol. Phys. **98**, 1213 (2000).
  - [8] S. Majumder and B. P. Das, Phys. Rev. A **62**, 042508 (2000).
  - [9] M. F. Gu, At. Data Nucl. Data Tables **89**, 267 (2005).
  - [10] H. C. Ho, W. R. Johnson, S. A. Blundell, and M. S. Safronova, Phys. Rev. A **74**, 022510 (2006).
  - [11] K. T. Cheng, M. H. Chen, and W. R. Johnson, Phys. Rev. A **77**, 052504 (2008).
  - [12] J. M. Sampaio, F. Parente, C. Nazé, M. Godefroid, P. Indelicato, and J. P. Marques, Phys. Scr. **T156**, 014015 (2013).
  - [13] V. A. Yerokhin, A. Surzhykov, and S. Fritzsche, Phys.

- Rev. A **90**, 022509 (2014).
- [14] K. Wang, X. L. Guo, H. T. Liu, D. F. Li, F. Y. Long, X. Y. Han, B. Duan, J. G. Li, M. Huang, Y. S. Wang, R. Hutton, Y. M. Zou, J. L. Zeng, C. Y. Chen, and J. Yan, *Astrophys. J. Suppl. Ser.* **218**, 16 (2015).
  - [15] A. A. El-Maaref, S. Schippers, and A. Müller, *Atoms* **3**, 2 (2015).
  - [16] K. K. Li, L. Zhuo, C. M. Zhang, C. Chen, and B. C. Gou, *Can. J. Phys.* **95**, 720 (2017).
  - [17] B. Edlén, *Phys. Scr.* **28**, 51 (1983).
  - [18] G. Möller, E. Träbert, V. Lodwig, C. Wagner, P. H. Heckmann, J. H. Blanke, A. E. Livingston, and P. H. Mokler, *Z. Phys. D* **11**, 333 (1989).
  - [19] E. Träbert, G. Möller, P. H. Heckmann, and A. E. Livingston, *Phys. Scr.* **41**, 860 (1990).
  - [20] G. Möller, E. Träbert, P. H. Heckmann, P. H. Mokler, and A. E. Livingston, *Z. Phys. D* **18**, 223 (1991).
  - [21] R. Büttner, B. Kraus, K. H. Scharfner, F. Folkmann, P. H. Mokler, and G. Möller, *Z. Phys. D* **22**, 693 (1992).
  - [22] P. Beiersdorfer, D. Knapp, R. E. Marrs, S. R. Elliott, and M. H. Chen, *Phys. Rev. Lett.* **71**, 3939 (1993).
  - [23] P. Beiersdorfer, A. Osterheld, S. R. Elliott, M. H. Chen, D. Knapp, and K. Reed, *Phys. Rev. A* **52**, 2693 (1995).
  - [24] E. Träbert, P. Beiersdorfer, J. K. Lepson, and H. Chen, *Phys. Rev. A* **68**, 042501 (2003).
  - [25] I. Draganić, J. R. Crespo López-Urrutia, R. DuBois, S. Fritzsche, V. M. Shabaev, R. Soria Orts, I. I. Tupitsyn, Y. Zou, and J. Ullrich, *Phys. Rev. Lett.* **91**, 183001 (2003).
  - [26] D. Feili, B. Zimmermann, C. Neacsu, P. Bosselmann, K.-H. Scharfner, F. Folkmann, A. E. Livingston, E. Träbert, and P. H. Mokler, *Phys. Scr.* **71**, 48 (2005).
  - [27] S. Schippers, D. Bernhardt, A. Müller, M. Lestinsky, M. Hahn, O. Novotný, D. W. Savin, M. Grieser, C. Krantz, R. Repnow, and A. Wolf, *Phys. Rev. A* **85**, 012513 (2012).
  - [28] D. Bernhardt, C. Brandau, Z. Harman, C. Kozhuharov, S. Böhm, F. Bosch, S. Fritzsche, J. Jacobi, S. Kieslich, H. Knopp, F. Nolden, W. Shi, Z. Stachura, M. Steck, Th. Stöhlker, S. Schippers, and A. Müller, *J. Phys. B: At. Mol. Opt. Phys.* **48**, 144008 (2015).
  - [29] A. V. Malyshev, A. V. Volotka, D. A. Glazov, I. I. Tupitsyn, V. M. Shabaev, and G. Plunien, *Phys. Rev. A* **90**, 062517 (2014).
  - [30] A. V. Malyshev, A. V. Volotka, D. A. Glazov, I. I. Tupitsyn, V. M. Shabaev, and G. Plunien, *Phys. Rev. A* **92**, 012514 (2015).
  - [31] W. H. Furry, *Phys. Rev.* **81**, 115 (1951).
  - [32] J. Sapirstein and K. T. Cheng, *Phys. Rev. A* **64**, 022502 (2001).
  - [33] J. Sapirstein and K. T. Cheng, *Phys. Rev. A* **63**, 032506 (2001).
  - [34] J. Sapirstein and K. T. Cheng, *Phys. Rev. A* **66**, 042501 (2002).
  - [35] J. Sapirstein and K. T. Cheng, *Phys. Rev. A* **67**, 022512 (2003).
  - [36] M. H. Chen, K. T. Cheng, W. R. Johnson, and J. Sapirstein, *Phys. Rev. A* **74**, 042510 (2006).
  - [37] J. Sapirstein and K. T. Cheng, *Phys. Rev. A* **74**, 042513 (2006).
  - [38] V. A. Yerokhin, A. N. Artemyev, and V. M. Shabaev, *Phys. Rev. A* **75**, 062501 (2007).
  - [39] A. N. Artemyev, V. M. Shabaev, I. I. Tupitsyn, G. Plunien, and V. A. Yerokhin, *Phys. Rev. Lett.* **98**, 173004 (2007).
  - [40] Y. S. Kozhedub, A. V. Volotka, A. N. Artemyev, D. A. Glazov, G. Plunien, V. M. Shabaev, I. I. Tupitsyn, and Th. Stöhlker, *Phys. Rev. A* **81**, 042513 (2010).
  - [41] J. Sapirstein and K. T. Cheng, *Phys. Rev. A* **83**, 012504 (2011).
  - [42] A. N. Artemyev, V. M. Shabaev, I. I. Tupitsyn, G. Plunien, A. Surzhykov, and S. Fritzsche, *Phys. Rev. A* **88**, 032518 (2013).
  - [43] A. V. Malyshev, D. A. Glazov, A. V. Volotka, I. I. Tupitsyn, V. M. Shabaev, G. Plunien, and Th. Stöhlker, *Phys. Rev. A* **96**, 022512 (2017).
  - [44] V. A. Yerokhin, A. N. Artemyev, and V. M. Shabaev, *Phys. Lett. A* **234**, 361 (1997).
  - [45] V. M. Shabaev, *Phys. Rep.* **356**, 119 (2002).
  - [46] M. A. Braun, A. D. Gurchumelia, and U. I. Safronova, *Relativistic Theory of Atom*, Nauka, Moscow, 1984.
  - [47] V. A. Yerokhin, A. N. Artemyev, T. Beier, G. Plunien, V. M. Shabaev, and G. Soff, *Phys. Rev. A* **60**, 3522 (1999).
  - [48] A. N. Artemyev, T. Beier, G. Plunien, V. M. Shabaev, G. Soff, and V. A. Yerokhin, *Phys. Rev. A* **60**, 45 (1999).
  - [49] V. A. Yerokhin, A. N. Artemyev, V. M. Shabaev, M. M. Sysak, O. M. Zherebtsov, and G. Soff, *Phys. Rev. A* **64**, 032109 (2001).
  - [50] É.-O. Le Bigot, P. Indelicato, and V. M. Shabaev, *Phys. Rev. A* **63**, 040501(R) (2001).
  - [51] A. N. Artemyev, T. Beier, G. Plunien, V. M. Shabaev, G. Soff, and V. A. Yerokhin, *Phys. Rev. A* **62**, 022116 (2000).
  - [52] A. N. Artemyev, V. M. Shabaev, V. A. Yerokhin, G. Plunien, and G. Soff, *Phys. Rev. A* **71**, 062104 (2005).
  - [53] Y. S. Kozhedub, A. V. Malyshev, D. A. Glazov, V. M. Shabaev, and I. I. Tupitsyn, *Phys. Rev. A* **100**, 062506 (2019).
  - [54] A. V. Malyshev, Y. S. Kozhedub, D. A. Glazov, I. I. Tupitsyn, and V. M. Shabaev, *Phys. Rev. A* **99**, 010501(R) (2019).
  - [55] V. F. Bratzev, G. B. Deyneka, and I. I. Tupitsyn, *Bull. Acad. Sci. USSR, Phys. Ser.* **41**, 173 (1977).
  - [56] I. I. Tupitsyn, V. M. Shabaev, J. R. Crespo López-Urrutia, I. Draganić, R. Soria Orts, and J. Ullrich, *Phys. Rev. A* **68**, 022511 (2003).
  - [57] M. Y. Kaygorodov, Y. S. Kozhedub, I. I. Tupitsyn, A. V. Malyshev, D. A. Glazov, G. Plunien, and V. M. Shabaev, *Phys. Rev. A* **99**, 032505 (2019).
  - [58] V. M. Shabaev, I. I. Tupitsyn, K. Pachucki, G. Plunien, and V. A. Yerokhin, *Phys. Rev. A* **72**, 062105 (2005).
  - [59] V. A. Yerokhin and V. M. Shabaev, *J. Phys. Chem. Ref. Data* **44**, 033103 (2015).
  - [60] V. M. Shabaev, I. I. Tupitsyn, and V. A. Yerokhin, *Phys. Rev. A* **88**, 012513 (2013).
  - [61] V. M. Shabaev, I. I. Tupitsyn, and V. A. Yerokhin, *Comp. Phys. Comm.* **223**, 69 (2018).
  - [62] I. I. Tupitsyn, M. G. Kozlov, M. S. Safronova, V. M. Shabaev, and V. A. Dzuba, *Phys. Rev. Lett.* **117**, 253001 (2016).
  - [63] L. F. Pašteka, E. Eliav, A. Borschevsky, U. Kaldor, and P. Schwerdtfeger, *Phys. Rev. Lett.* **118**, 023002 (2017).
  - [64] V. A. Yerokhin, A. Surzhykov, and A. Müller, *Phys. Rev. A* **96**, 042505 (2017).
  - [65] J. Machado, C. I. Szabo, J. P. Santos, P. Amaro, M. Guerra, A. Gumberidze, Guojie Bian, J. M. Isac,

- and P. Indelicato, Phys. Rev. A **97**, 032517 (2018).
- [66] V. A. Zaytsev, I. A. Maltsev, I. I. Tupitsyn, and V. M. Shabaev, Phys. Rev. A **100**, 052504 (2019).
- [67] V. M. Shabaev, I. I. Tupitsyn, M. Y. Kaygorodov, Y. S. Kozhedub, A. V. Malyshev, and D. V. Mironova, Phys. Rev. A **101**, 052502 (2020).
- [68] P. J. Mohr, D. B. Newell, and B. N. Taylor, Rev. Mod. Phys. **88**, 035009 (2016).